ALKALI METALS ON III-V (110) SEMICONDUCTOR SURFACES: OVERLAYER PROPERTIES AND MANIPULATION VIA STM

L. J. WHITMAN
Naval Research Laboratory
Washington, DC 20375 USA

JOSEPH A. STROSCIO, R. A. DRAGOSET, and R. J. CELOTTA
National Institute of Standards and Technology,
Gaithersburg, MD 20899 USA

ABSTRACT: Field ion microscopists demonstrated more than twenty years ago that polarizable atoms adsorbed on a stepped surface can be induced to diffuse by an electric field due to the field gradients associated with step edges. We have exploited a similar phenomenon, the large field gradients in the vicinity of the STM tip, to induce the directional diffusion of Cs and K atoms adsorbed on room temperature GaAs(110) and InSb(110). The geometric and electronic properties of both the naturally occurring and electric field-induced alkali metal structures observed on these semiconductor surfaces are discussed, including the possibility that the alkali metal overlayers are Mott insulators.

1. Introduction

The rapid growth in the number of operational scanning tunneling microscopes (STM) has been accompanied by many attempts to use the STM for nanoscale modification of surfaces [1]. There are four fundamental processes inherent to surface modification: removal of surface atoms; deposition of new material; lateral translation of adsorbed atoms; and induction of local chemistry (e.g. dissociation of an adsorbate or reaction between adjacent adsorbates). In order to achieve these modifications the scanning tunneling microscopist has three basic parameters to vary: the tip properties, including the material composition of the tip and the tip shape; the tunneling current, which can be varied via the tunneling gap or the tunneling bias; and the electric field in the tunnel junction, which is also dependent on the gap and bias.

A few examples from the recent literature elucidate how the above three parameters have been employed, usually in combination, to perform nanoscale surface modification with an STM. For instance, Lyo and Avouris have recently demonstrated the removal of surface atoms (small Si clusters) from Si(111) [2]. The process appears to depend on a combination of the electric field (field evaporpation) and the tip properties (via direct tip-surface interaction). The recent work of Mamin, Guethner, and Ruger provides a nice example of controlled deposition of material (Au) from tip to surface [3], with the deposition appearing to depend primarily on the electric field,

P. Avouris (ed.), Atomic and Nanometer-Scale Modification of Materials: Fundamentals and Applications, 25–35.

although local heating due to the high current densities in the junction may also play a role [4]. Lateral translation of adsorbed atoms via the STM has been precisely demonstrated in the experiments of Eigler and Schweizer with Xe at 4 K, with the process dependent on the tip properties [5]. The high electric field and current density in the tunnel junction is a useful combination for the induction of local chemistry, such as the dissociation of individual decaborane molecules achieved on Si(111) [6].

In this paper we review our progress in using the electric field in the STM tunnel junction to translate adsorbed atoms (Cs and K) across the (110) surfaces of GaAs and InSb at room temperature [7]. Field ion microscopists demonstrated more than twenty years ago that polarizable atoms adsorbed on a stepped surface can be induced to diffuse by an electric field due to the field gradients that occur in the vicinity of the step edges [8-10]: we have exploited the large field gradients in the vicinity of the STM tip to induce a similar directional diffusion of these alkali metal adatoms. In addition, we have used the STM to explore the geometric and electronic properties of both the naturally occurring and induced structures [11-13]. Here we will first discuss the naturally occurring structures, then electric field-induced diffusion, and lastly the electronic properties of the observed structures. All experiments were performed in ultra-high vacuum at room temperature, as previously described [11-13]. Note that all STM images shown are of the filled electronic states (tunneling from surface to tip).

2. Results and Discussion

2.1 NATURALLY OCCURRING STRUCTURES

Cs and K adsorbed on room temperature GaAs(110) and InSb(110) form a variety of interesting structures, evolving from one- to two- to three-dimensional (3-D) with increasing coverage [11-13]. Following the adsorption of low coverages long 1-D chains oriented along the $[1\bar{1}0]$ direction are observed, as illustrated by the STM images of Cs on InSb(110) shown in Fig. 1. For Cs on both substrates and K on GaAs(110) these chains have a characteristic zig-zag structure, with the adatoms appearing to be adsorbed in the four-fold hollow-like sites between the substrate anions (As, Sb). The formation of these 1-D chains is consistent with the highly anisotropic barrier to diffusion: the calculated barrier along the $[1\bar{1}0]$ direction (0.2 eV) is approximately one fifth that expected along [001] (1.0 eV) [14]. However, this does not readily account for the unusual zig-zag structure within the chains. One factor in determining the internal structure of the chains may be the lattice mismatches between Cs (bulk nearest-neighbor distance a=0.52 nm) and GaAs(110) and InSb(110) (unit cell size along $[1\bar{1}0]$ a=0.40 nm and a=0.46 nm, respectively). The Cs atoms will not readily fit in adjacent hollows along $[1\bar{1}0]$ on these substrates. This is also true of K (a=0.46 nm) on GaAs(110).

In contrast to Cs and K on GaAs(110) and Cs on InSb(110), K is latticed-matched with InSb(110) and should therefore fit in every hollow along a 1-D chain. However, as observed in Fig. 2, although K also forms 1-D chains on InSb(110) the chains are a single atom wide with K atoms adsorbed in *every-other* hollow. Furthermore, the atomic-resolution image of Fig. 2(b) reveals substantial in-plane relaxation of the substrate Sb atoms surrounding each K atom, with the adjacent Sb atoms appearing to relax away from each K adatom. This has the effect of making the hollow sites adjacent to each adatom smaller than normal, which could result in the alternate spacing of the adatoms within each chain. Careful analysis of the apparent substrate anion atomic positions surrounding the Cs and K zig-zag chains reveals similar, although

smaller, in-plane relaxations associated with these chains also. These results demonstrate that in addition to any kinetic effects associated with the initial formation of these 1-D chains, the alkali metal-substrate interactions also play an important role in determining the ultimate chain structures [14,15].

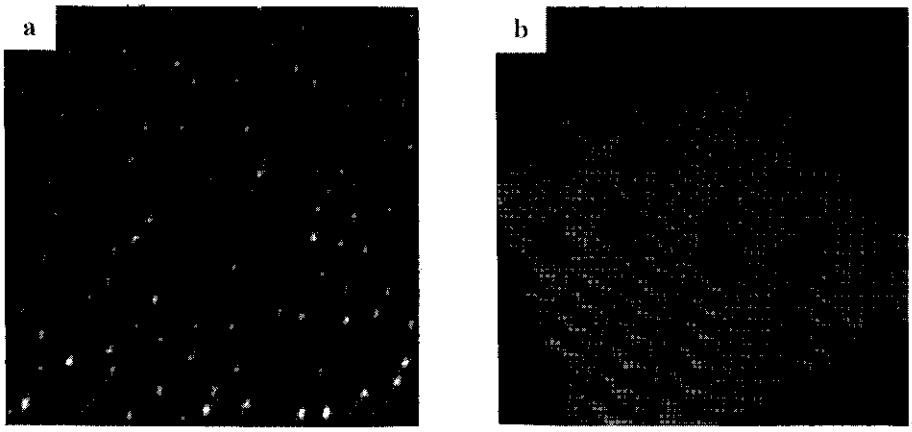

FIG. 1. STM topographic images of naturally occurring Cs zig-zag chains on InSb(110), with a Cs coverage ≈0.08 per substrate unit cell, recorded with negative sample bias. The chains run along the [1$\bar{1}$0] direction. (a) 60×60 nm^2 gray-scale view. (b) 12.5×12.5 nm^2 solid-rendered view with atomic resolution. Note that the substrate corrugation is due to the Sb atoms only at this bias voltage. The gray scale spans a range ≈0.15 nm.

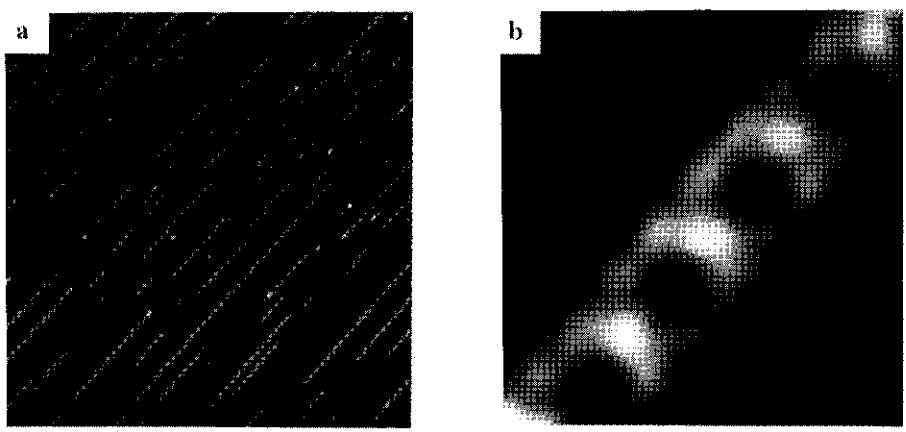

FIG. 2. Gray-scale topographic images of 1-D K chains on InSb(110). (a) 120×120 nm^2. (b) 3.5×3.5 nm^2 atomic-resolution view of a chain section. The brightest atomic-scale features appearing in every other hollow-like site along [1$\bar{1}$0] are believed to correspond to the K adatoms. Note the in-plane relaxation of the adjacent Sb atoms, observed as a slight dimerization along [1$\bar{1}$0], particularly along the chain and in the lower right corner of the image.

Following further adsorption of Cs or K on these substrates, the chains do not tile the surface, but rather become unstable, breaking up into disordered clusters. With increasing coverage the overlayers evolve into ordered 2-D structures composed of arrays of alkali metal (110)-like planar clusters. As previously reported [12,13], Cs forms a c(4×4) overlayer of five-atom clusters on GaAs(110) and a c(2×6) overlayer of four-atom clusters on InSb(110). We find that K forms a similar c(2×6) overlayer on both substrates, as shown for K on GaAs(110) in Fig. 3(a). Although the structure within the planar K clusters has not yet been resolved, the clusters appear to have the same four-atom structure as that observed for Cs on InSb(110), an atomic-resolution image of which is displayed in Fig. 3(b). Both the four- and five-atom planar clusters have an internal structure similar to that of an alkali metal bcc (110) surface [12,13]. In addition, these structures are close to those predicted to be stable for gas phase clusters of the same size [16]. These two observations indicate that the 2-D structures result from a balance between adsorbate-adsorbate interactions (which drive the formation of bulk-like clusters) and adsorbate-substrate interactions (which induce the commensurate superstructure).

When the 2-D overlayers are exposed to additional alkali metal, further adsorption occurs on top of the intial overlayers in a random fashion [12,13]. Since the first layer is not epitaxial, and the second layer has little interaction with the substrate, there is no mechanism for the formation of long-range order. The saturation structure observed for Cs or K adsorbed on either room temperature GaAs(110) or InSb(110) is a disordered bilayer.

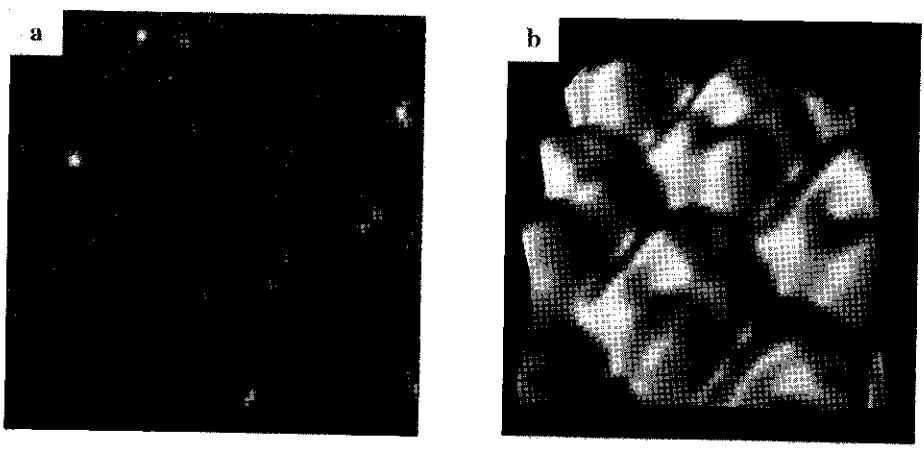

FIG. 3. 2-D alkali metal overlayers on InSb(110). (a) 40×40 nm^2 gray-scale image of a K overlayer. Each maximum in the image is a planar K cluster. The closely packed regions have a c(2×6) symmetry. (With slightly higher coverage the whole surface has this structure.) (b) 3×3 nm^2 solid-rendered view of similar Cs clusters with atomic resolution. The clusters appear to have four Cs atoms each.

2.2 FIELD-INDUCED DIRECTIONAL DIFFUSION

An atom or molecule with a static dipole moment μ and polarizability α placed in an electric field $\mathbf{E}(\mathbf{r})$ will have an induced dipole moment $\alpha\mathbf{E}$, and will experience a potential energy due to the field

$$U_E(\mathbf{r}) \cong -\mu \cdot \mathbf{E}(\mathbf{r}) - \tfrac{1}{2}\alpha\mathbf{E}(\mathbf{r}) \cdot \mathbf{E}(\mathbf{r}) . \qquad (1)$$

If the electric field varies as a function of $\mathbf{r}$, the atom or molecule will experience a potential energy gradient (that is, a force). Field ion microscopists have exploited this phenomenon to induce the directional diffusion of metal atoms adsorbed on the surfaces of field ion microscope (FIM) tips [8-10]. In an FIM a sharp tip, usually of refractory metal, terminated by a series of stacked low-index crystal planes is held a few centimeters away from an imaging plane at an electrostatic potential difference of many kilovolts. The electric fields at the surfaces on the end of the tip are typically 10^7 - 10^8 V cm^{-1}, with the intensity varying across each crystal terrace and enhanced near the terrace edges (due to the high curvature associated with a surface step). As a result of the field gradients near the step edges, adatoms with a positive static dipole in a positive electric field undergo thermally activated directional diffusion towards the region of greatest field (the terrace edge) [9,10]. For the transition metal adatoms studied in the FIM experiments, the induced dipole moments are typically an order of magnitude smaller than the static dipole moments ($\mu \sim 10^{-27}$ C cm), so the potential energy is dominated by the first term in Eq. (1) [9,10]. Hence the adatoms can be induced to diffuse toward or away from the step edges depending on whether the electric field is positive or negative, respectively.

In an STM the same ingredients necessary for electric field-induced directional diffusion are present, except that the electric field now results from having a sharp tip with an electrostatic potential difference of a few volts located less than a nanometer above the surface under study. In the STM the electric field intensity at the sample surface decreases with increasing radial distance from the end of the tip. For example, on a metal surface the field will fall to about half its maximum value at a distance approximately equal to the radius of the end of the tip [7]. Therefore, an adatom with a positive dipole moment on a surface at positive potential with respect to the tip will experience a potential energy well under the tip, and directionally diffuse towards the tip while the field is applied. (Recall that this is a thermally activated process.)

We have observed such diffusion for both Cs and K on room temperature GaAs and InSb (110) surfaces. As will be discussed in more detail below, the surfaces can be imaged with negative bias voltage without any apparent effect on the substrate or adsorbate overlayer. If the tip is positioned over the center of a previously imaged area and the sample bias is temporarily changed from negative to positive, subsequent images (with negative bias) reveal an increase in the alkali metal concentration in the region beneath the tip, as expected. One such sequence is presented in Fig. 4, showing a region of a GaAs (110) surface covered with Cs chains before and after a 0.35 s, +1 V pulse. As previously reported [7], during the voltage pulse alkali metal adatoms diffuse into the region beneath the tip, resulting in an increase in the number of alkali metal chains in the region, a shift in the chain length distribution towards longer chains, and an overall increase in local coverage. In general, the longer the positive bias is applied the greater the increase in local alkali metal coverage, as expected for a diffusion process. The effects of the induced diffusion, such as the appearance of new and longer alkali metal chains, are consistent

with our understanding of the kinetics and thermodynamics that lead to the formation of 1-D chains following the initial adsorption (in the absence of an electric field).

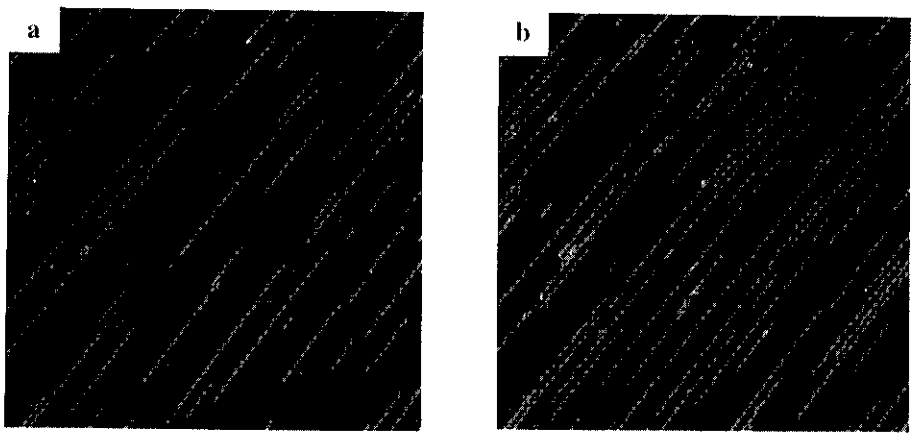

FIG. 4. Images of Cs chains in a 140×140 nm^2 area of *p*-type GaAs(110) recorded with negative sample bias (a) before, and (b) after positioning the tip over the center of the area and changing the bias to +1 V for 0.35 s.

The local effects of electric field-induced diffusion with the STM can be very dramatic, as illustrated by the images in Fig. 5. Prior to applying a 0.35 s, +3 V pulse, the area of GaAs(110) shown in Fig. 5(a) was covered with a uniformly sparse distribution of short (<20 nm) Cs chains. After inducing diffusion into the center of the imaged area, a region a few tens of nanometers across with very high local coverage is observed. Surprisingly, closer examination of this region reveals that a new 2-D phase has been created, an atomic-resolution image of which is displayed in Fig. 5(b). Unlike the naturally occurring 2-D phase for this system, composed of a c(4×4) array of five-atom planar clusters, this newly created phase of adsorbed Cs is primarily a c(2×2) arrangement of individual adatoms. Other, less well ordered structures that also do not naturally occur following room temperature adsorption have been created in this way on InSb(110) [7]. This demonstrates the potential of this technique to create and study novel configurations of adsorbed atoms and molecules at room temperature.

Although we have only briefly reviewed our results here, there are a number of puzzling observations worthy of discussion. The most striking observation is probably the polarity dependence of the directional diffusion; that is, diffusion occurs with a positive sample bias, but no apparent field effects are observed with the negative voltages typically used to obtain images of the filled states (–2 to –3 V). This is in contrast to the reversible directional diffusion observed in FIM, as discussed above. The explanation for the polarity dependence we observe lies in the relatively large polarizability of the alkali metal adatoms, and the resulting potential energy as expressed in Eq. (1). The polarizability of a Cs atom adsorbed on GaAs(110) is expected to be of similar magnitude to that of the free atom, ~1×10^{-34} C cm^2 V^{-1} (100 Å^3) [17]. With such a polarizability, a static dipole moment $\mu \approx 1.6\times10^{-27}$ C m (as determined from the initial decrease in work function upon Cs adsorption [18]), and a sample bias of +3 V with a

tunnel gap of 1 nm, a Cs adatom would experience a potential energy well ≈0.6 eV deep, with the static and induced dipoles both contributing equally beneath the tip. This is sufficiently deep compared with the expected diffusion barrier along [1$\bar{1}$0] to account for the directional diffusion we observe. In contrast, when the bias is reversed to –3 V, although the static dipole now leads to a *repulsive* potential energy barrier, the potential due to the induced dipole moment remains an *attractive* energy well. The net field-induced potential energy is approximately zero beneath the tip, accounting for the absence of induced diffusion under these conditions. Note that at larger negative voltages the induced dipole should dominate, making the potential energy again attractive. We have seen some evidence for diffusion towards the tip at –5 to –6 V, consistent with this expectation, although the results are inconclusive.

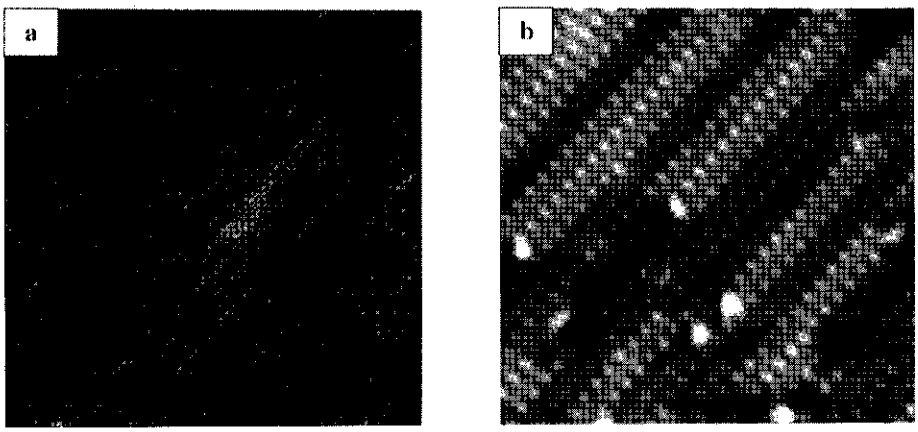

FIG. 5. The effect of a 0.35 s, +3 V pulse on Cs chains on *p*-type GaAs(110). (a) The 350×350 nm^2 region surrounding the pulse location. Prior to the pulse the region was sparsely covered with short Cs chains. (See Ref. [7].) (b) A 20×20 nm^2 image of the high-density area at the pulse location. This structure, which has a local c(2×2) symmetry, is not normally observed on GaAs(110).

In addition to the dependence on field polarity, on GaAs(110) we also observe a dependence of the threshold voltage (for observable diffusion) on sample dopant type (*n* versus *p*). While on *p*-type GaAs a sample bias of approximately +0.5 V is required to induce observable diffusion, a +2.0 V bias is necessary with *n*-type. This observation can be accounted for on the basis of the diclectric properties of the semiconductor, which allow the electric field to penetrate into the surface (band bending). Band bending has the effect of reducing the potential difference between the surface and the tip, thereby reducing the electric field at the surface and any resulting directional diffusion. With a *p*-type GaAs substrate at positive bias, upward band bending is limited by the creation of an inversion layer. In contrast, with an *n*-type substrate the bands can be bent upward through the bulk band gap, 1.45 eV, thereby decreasing the effective surface voltage by this amount [19].

The final observation which we will discuss is the large collection area beneath the tip observed on GaAs(110). Based on the electric field profile on a metal surface, the potential energy well beneath the tip is expected to be approximately a tip diameter wide. (Scanning

electron micrographs show our tips to be typically 20-40 nm in diameter.) However, the alkali metal adatom concentration increases within a region substantially wider than this on GaAs(110). We believe this also arises from the large field penetration that occurs on this wide band gap semiconductor, since such penetration will modulate both the magnitude and radial dependence of the electric fields perpendicular to the surface. Furthermore, this penetration will give rise to a component of the electric field *parallel* to the surface. Since the parallel polarizability of the Cs adatoms within 1-D chains is predicted to be even larger than that normal to the surface [17], an in-plane component of the field could contribute significantly to the potential energy gradient on this semiconductor surface.

2.3 ELECTRONIC PROPERTIES

In addition to characterizing the geometric properties of the naturally occurring and electric field-induced alkali metal structures, we have also investigated their electronic properties by measuring the voltage dependence of the tunneling current (*I-V* spectra) as a function of structure [12,13]. A comparison of typical *I-V* spectra recorded over 1- 2- and 3-D Cs structures on GaAs(110) and InSb(110) is displayed in Fig. 6. The apparent band gap associated with a 1-D zig-zag chain on GaAs(110) is ≈1.1 eV, indicating that these chains are not 1-D "wires." (We define the apparent band gap as the region of a spectrum with zero conductivity.) Note that the *I-V* spectrum recorded over a similar 1-D chain on InSb(110) has a much smaller gap width, ≈0.15 eV, approximately equal to the InSb band gap. We believe this is not necessarily a measure of the "chain gap," however, but rather an indication that tunneling is occurring into and out of the substrate states due to the open structure of the chain [13]. Similar results are obtained when spectra are recorded over 1-D K chains.

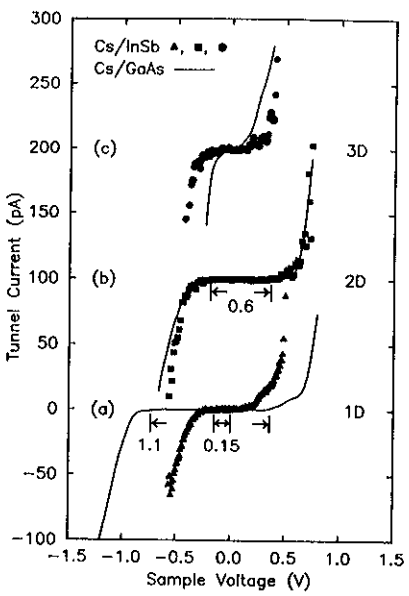

FIG. 6. A comparison of current vs voltage spectra recorded on various Cs structures on GaAs(110) (lines) and InSb(110) (symbols): (a) 1-D zig-zag chain; (b) 2-D overlayer; (c) 3-D saturation bilayer (see Refs. [12] and [13]). The band gaps indicated correspond to the regions of zero conductivity, determined on a more sensitive scale. Note that the GaAs spectra have been slightly smoothed, and that the spectra in (b) and (c) are offset from zero current.

The comparison between the electronic properties of the similar 2-D Cs overlayers on GaAs(110) and InSb(110), shown in spectra (b), reveals one of the most surprising results of our study: alkali metal monolayers on III-V (110) semiconductor surfaces are nonmetallic and have nearly identical *I-V* characteristics, with a characteristic band gap ≈0.6 eV. This is true not only for the 2-D Cs overlayers, but for the 2-D K overlayers *and* the novel 2-D structures created via field-induced diffusion. This result is particularly striking for the case of InSb(110), where the overlayers open up an apparent gap *larger* than the substrate band gap. It is not until the formation of 3-D structures near saturation coverage (the disordered bilayers) that the measured gap narrows and these overlayers become metallic or near-metallic [spectra (c)].

An intriguing explanation for the unusual coverage dependence of the electronic properties of the alkali metal overlayers is that the 1-D and 2-D structures are Mott insulators [12,13,20]. If this is the case, the nonmetallic behavior arises from electron correlation effects caused by the low alkali metal density and coordination within these structures: the reduced electron wave function overlap between atoms as compared to that within bulk 3-D structures causes the electronic structure to remain atomic-like. The resulting coulomb repulsion between electrons (known as a correlation effect) creates a barrier to electron transport within the structures (the correlation energy), which we observe as a "band gap" in the *I-V* spectra. As the density and coordination increase with increasing dimensionality and the wave function overlap increases, the correlation energy decreases, lowering the observed gap. When 3-D structures form, with bulk-like density and coordination, a metallic band structure develops and the gaps in the spectra vanish. Note that a similar insulator-to-metal Mott transition occurs as a function of density in liquid alkali metals [21], supporting this explanation. In addition, recent band structure calculations for model alkali metal overlayers on GaAs(110) also offer evidence that electron correlation effects play a role in the electronic structure [14,22].

Although there is some support for the description of these systems as Mott insulators, an alternate explanation for their unexpected electronic properties may be offered in terms of more conventional band structure effects [13]. The similar chemical properties of the different alkali metals combined with the similar properties of the different III-V (110) semiconductor surfaces may result in a characteristic alkali metal-III-V(110) interface band structure for each similar interface structure. If this is the case, adsorbate-substrate interactions must be responsible for changing the electronic structure of the alkali metal overlayers from an expected metallic state to the observed insulating state. Note that there is at least one system exhibiting such behavior, the (1×1) Sb overlayer on GaAs(110): the isolated Sb overlayer is predicted to be metallic but the measured (and calculated) interface band structure is not [23-25]. Further experimental and theoretical work is required to resolve which mechanisms are responsible for the interesting electronic properties of these alkali metal overlayers [13].

3. Summary and Conclusions

The alkali metals (Cs and K) adsorbed on room temperature III-V (110) semiconductor surfaces (GaAs and InSb) form a rich variety of structures with surprising electronic properties. With low coverages 1-D chains oriented along $[1\bar{1}0]$ are observed. These structures can be accounted for on the basis of anisotropic diffusion kinetics combined with the effects of adsorbate-substrate interaction. The 1-D chains are not metallic, with a gap in the *I-V* spectra observed for all chain types. At higher coverages the 1-D chains give way to ordered 2-D structures composed of

arrays of alkali metal (110)-like planar clusters, showing the effects of both interadsorbate and adsorbate-substrate interactions. The 2-D overlayers all have nearly identical *I-V* characteristics, with an apparent band gap of ≈0.6 eV. Remarkably, on InSb(110) the 2-D alkali metal overlayers open up a gap *larger* than that of the substrate. At the highest attainable coverages at room temperature the absence of an epitaxial first layer results in the growth of disordered 3-D bilayers, with metallic or near-metallic characteristics. The evolution of the electronic structure with increasing dimensionality is consistent with the alkali metal overlayers behaving as Mott insulators. However, the electronic properties may alternately be attributed to simpler interface band structure effects. A more definitive explanation requires further investigation.

We have used the nonuniform electric field in the STM tunnel junction to induce the directional diffusion of the alkali metal adatoms toward the tip when a positive sample bias is applied. This thermally activated directional diffusion arises from the potential energy gradient created by the interaction of the static and induced dipole moments of the adatoms with the spatially varying electric field surrounding the tip. The absence of field-induced effects with negative bias (with which the images were recorded) can be attributed to the relatively large, free-atom-like polarizability of the alkali metal atoms when adsorbed on these semiconductor surfaces. The response of these systems to an applied electric field appears to be strongly affected by the dielectric properties of the semiconductor, in particular by the occurrence of band bending.

In the FIM, electric field-induced directional diffusion has been demonstrated for a variety of metal adatoms on FIM tip surfaces [8-10]. Given that electric fields of similar magnitudes are attainable in the STM tunnel junction, directional diffusion of a variety of polarizable atoms and molecules should be possible on semiconductor (and metal) surfaces other than those studied here. Of course an important caveat to this prediction is that one must always be on the lookout for unintended electric field-induced effects when studying surfaces with the STM, particularly in the presence of adsorbates with large static dipole moments or polarizabilities.

It is clear from this and other studies that the STM, along with the other scanned probe-type instruments, has great potential for controlled nanoscale modification of materials. If nanoelectronic devices fabricated via STM are ever to be employed in practical applications, however, at least two major hurdles must be overcome: the problem of interconnectivity - how can nanoscale devices be connected to more conventional circuit elements (without altering their properties)? and the problem of throughput - can such devices be fabricated reliably in parallel? While it is not certain whether STM-nanofabrication will soon lead to practical devices, it will clearly have a major impact probing the limits of miniaturization. The unprecedented ability to manipulate adsorbates into novel configurations, and subsequently study their geometric and electronic properties with the STM (or their mechanical and chemical properties with the atomic force microscope) should lead to a new understanding of how the fundamental properties of materials evolve atom-by-atom.

4. Acknowledgments

L. J. W. is grateful for the NRC-NIST Postdoctoral Fellowship which supported his work while at NIST. This work was also supported in part by the Office of Naval Research.

5. References

1. For recent reviews, see G. M. Shedd and P. E. Russell, Nanotechnology **1**, 67 (1990); C. F. Quate, in *Highlights in Condensed Matter Physics and Future Prospects*, edited by Leo Esaki (Plenum, New York, 1991), p. 573; and J. A. Stroscio and D. M. Eigler, Science **254**, 1319 (1991).
2. I.-W. Lyo and Ph. Avouris, Science **253**, 173 (1991).
3. H. J. Mamin, P. H. Guethner, and D. Rugar, Phys. Rev. Lett. **65**, 2418 (1990).
4. T. T. Tsong, Phys. Rev. B **44**, 13703 (1991).
5. D. M. Eigler and E. K. Schweizer, Nature **344**, 524 (1990).
6. G. Dujardin, R. E. Walkup, and Ph. Avouris, Science **255**, 1232 (1992).
7. L. J. Whitman, J. A. Stroscio, R. A. Dragoset, and R. J. Celotta, Science **251**, 1206 (1991).
8. E. V. Klimenko and A. G. Naumovets, Sov. Phys. Solid State **13**, 25 (1971) [Fiz. Tverd. Tela **13**, 33 (1971)]; Sov. Phys. Solid State **15**, 2181 (1974) [Fiz. Tverd. Tela **15**, 3273 (1973)].
9. T. T. Tsong and G. Kellogg, Phys. Rev. B **12**, 1343 (1975).
10. S. C. Wang and T. T. Tsong, Phys. Rev. B **26**, 6470 (1982).
11. L. J. Whitman, J. A. Stroscio, R. A. Dragoset, and R. J. Celotta, J. Vac. Sci. Technol B **9**, 770 (1991).
12. L. J. Whitman, J. A. Stroscio, R. A. Dragoset, and R. J. Celotta, Phys. Rev. Lett. **66**, 1338 (1991).
13. L. J. Whitman, J. A. Stroscio, R. A. Dragoset, and R. J. Celotta, Phys. Rev. B **44**, 5951 (1991).
14. J. Hebenstreit, M. Heinemann, and M. Scheffler, Phys. Rev. Lett. **67**, 1031 (1991).
15. K-induced relaxation of GaAs(110) is also discussed by C. A. Ventrice, Jr. and N. J. DiNardo, Phys. Rev. B **43**, 14313 (1991).
16. V. Bonacic-Koutecky, P. Fantucci, I. Boustani, and J. Koutecky, in *Studies in Physical and Theoretical Chemistry* (Elsevier, Amsterdam, 1989), Vol. 62, p. 429.
17. M. Krauss and W. J. Stevens, J. Chem, Phys. **93**, 8915 (1990).
18. Based on the results reported by D. Heskett, T. Maeda Wong, A. J. Smith, W. R. Graham, N. J. DiNardo, and E. W. Plummer, J. Vac. Sci. Technol. B **7**, 915 (1989).
19. R. M. Feenstra, J. A. Stroscio, and A. P. Fein, J. Vac. Sci. Technol. B **5**, 923 (1987).
20. N. J. DiNardo, T. Maeda Wong, and E. W. Plummer, Phys. Rev. Lett. **65**, 2177 (1990).
21. D. E. Logan and P. P. Edwards, in *The Metallic and Nonmetallic States of Matter*, edited by P. P. Edwards and C. N. R. Rao (Taylor & Francis, London, 1985), p. 78; W. Freyland and F. Hensel, *ibid*, p. 93, and references therein.
22. J. E. Klepeis, O. Pankratov, M. Scheffler, M. Methfessel, and M. Van Schilfgaarde, Bull. Am. Phys. Soc. **37**, 86 (1992).
23. R. M. Feenstra and P. Martensson, Phys. Rev. Lett. **61**, 447 (1988); P. Martensson and R. M. Feenstra, Phys. Rev. B **39**, 7744 (1989).
24. C. K. Shih, R. M. Feenstra, and P. Martensson, J. Vac. Sci. Technol A **8**, 3379 (1990).
25. C. Mailhiot, C. B. Duke, and D. J. Chadi, Phys. Rev. Lett. **53**, 2114 (1984); Phys. Rev. B **31**, 2213 (1985).